EFFECT OF MACRO-ROUGHNESS ELEMENTS ON TSUNAMI INUNDATION: SINK TERM FORMULAE FOR DEPTH-AVERAGED NUMERICAL MODELS

Stefan Leschka, DHI WASY GmbH, sle@dhigroup.com
Clemens Krautwald, TU Braunschweig, c.krautwald@tu-braunschweig.de
Hocine Oumeraci, TU Braunschweig, h.oumeraci@tu-braunschweig.de

INTRODUCTION

Tsunami propagation and inundation are commonly simulated using large-scale depth-averaged models. In such models, the quadratic friction law with a selected Manning's coefficient is generally applied to account for the effect of bottom surface roughness in each computational element. Buildings and tree vegetation in coastal areas are usually smaller than the computational element size. Using empirical Manning's coefficients to account for such large objects is not physically sound and, particularly in tsunami inundation modelling, this may result in large uncertainties. Therefore, an improved understanding of the processes associated with the hydraulic resistance of the so-called macro-roughness elements (MRE) is required. Relevant parameters such as shape, height and arrangement of the MRE should be investigated through laboratory experiments or numerical tests using a well-validated three-dimensional CFD model. Given the correlation of such parameters to the MRE-induced hydraulic resistance, empirical formulae were developed and directly implemented as sink terms in depth-averaged numerical solvers such as non-linear shallow-water (NLSW) models.

METHODOLOGY

An OpenFOAM® based 3D two-phase Reynolds-averaged Navier-Stokes (RANS) model including the volume of fluid (VOF) method is validated against data sets from five different laboratory experiments (Leschka et al., 2014). The performance of the 3D-CFD models are evaluated by means of non-dimensional statistical criteria for time series comparisons. A numerical test program with more than 20 simulations is developed, including the variation of the shape, arrangement, density and relative height of the MRE. The propagation of the bore is analyzed mainly based on the water content α of a computational cell and flow velocity u. They are integrated over the cross-section of each of the three segments along the MRE zone in Figure 1 to obtain volume flux $p(x)$ and flow depth h, which represent flow parameters typical in NLSW equations.

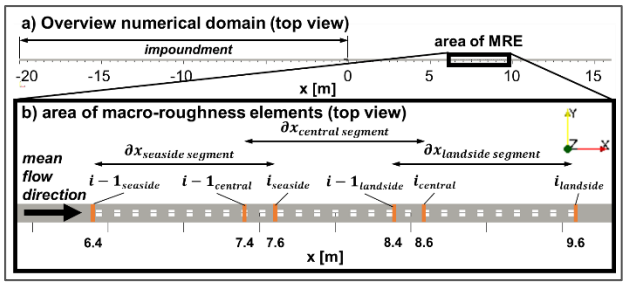

Figure 1 – Analyzed cross-sections in the area of macro-roughness elements. a) Overview of the numerical domain, b) area of macro-roughness elements.

Figure 2 illustrates the procedure to derive the sink terms. The data obtained from the validated CFD model was used to calculate the sink term for the so-called reference case without MRE, where only friction losses can be observed, and the cases with MRE (respectively Steps 1 and 2 in Figure 2). The difference between the results of the reference case S_f and the results of the cases with MRE S_{total} represents the sink term S_{MRE} associated with the MRE-induced energy losses (Step 3 in Figure 2). It can be calculated using

$$\frac{\partial p(x)}{\partial t} + \frac{\partial}{\partial x}\left[\frac{p(x)^2}{h} + gh^2 - \frac{h}{\rho}\tau_{xx}\right] - S_f = S_{MRE}$$
$$\approx S_{MRE,fit} = f(MRE\ parameters, flow\ parameters). \quad (1)$$

Dimensional analyses are performed to determine correlations of the sink term with Reynolds, Froude and Euler number. Furthermore, the correlations of the sink term with a characteristic length, the permeable cross-section, the flux derivative term and gravity derivative term of the NLSW equation (Step 4 in Figure 2) are analyzed.

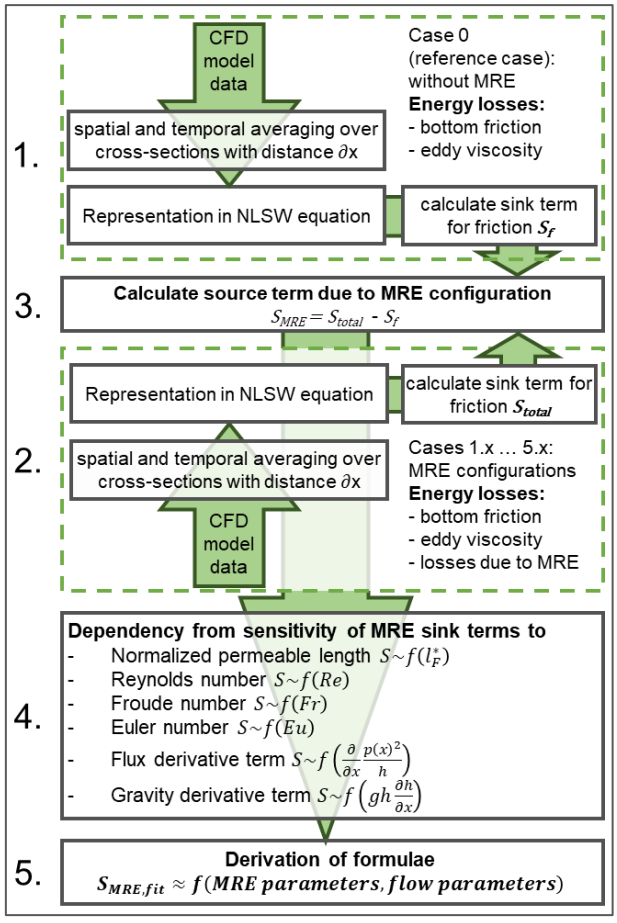

Figure 2 – Overview of the analysis procedure to derive a sink term $S_{MRE,fit}$ describing the energy losses due to MRE from data obtained from the CFD model.

By means of these quantities, multi-regression analyses "empirical" relationships are obtained (Step 5 in Figure 2),

which describe the effect of MRE arrangement (expressed by angle Ψ_B), relative MRE height h_B^*, distance between MRE (expressed by a normalized permeable length l_F^*) and MRE shape (expressed by drag coefficient C_D) on the sink term S_{MRE}.

These relationships are implemented in a NLSW model (COMCOT; Wang, 2008), and the results are compared with the laboratory experiments of Park, et al. (2013).

RESULTS

The dependency of the sink term from MRE parameters and flow characteristics (Step 4 in Figure 2) is expressed by means of two distinct times corresponding to: (1) high flow velocities (unsteady phase of bore propagation) and (2) large flow depths (steady phase). Exemplarily, the dependency of the sink term S_{MRE} from the normalized permeable length l_F^* for emerged MRE is shown in Figure 3.

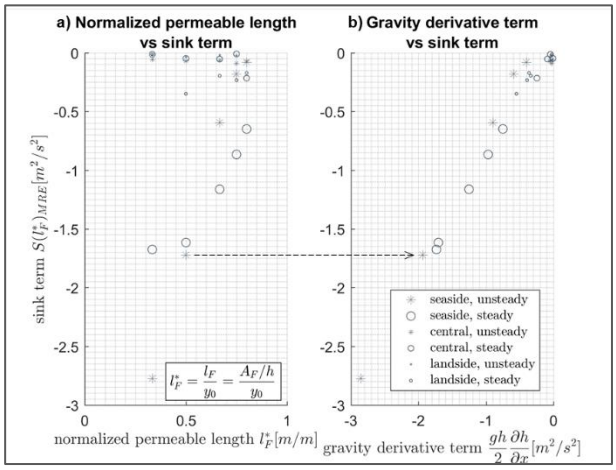

Figure 3 – Sink term $S(l_F^*)_{MRE}$ for various normalized permeable lengths l_F^*. a) normalized permeable length vs sink term, b) gravity derivative term vs sink term.

In Figure 3, A_F is the permeable cross-section area, which is not blocked by MRE (see Figure 1). It is related to a unit length y_0. In case of emerged MRE, l_F is the clearance between two neighboring MRE and l_F^* can then be interpreted as "porosity" of the cross-section. The results in Figure 3.a) reveal, for example, that the sink terms at the central and landside segments take considerably smaller values than at the seaside segments, which is due to the sheltering effect of the MRE in the first row of MRE, which cause a channeling of the flow. In the first row, the effect of the normalized permeable length on the sink term is stronger during the unsteady phase of the bore propagation.

The relationship between Figure 3.a) and Figure 3.b) is provided by equal y axes. In Figure 3.b), the strong dependency between the gravity derivative term and the sink term for various normalized permeable lengths can be seen. Therefore, the gravity derivative term was used to build the basis for the sink term fit. However, the normalized permeable length cannot directly be used in for the sink term formulae, as it is only an adequate measure for emerged MRE. Therefore, a characteristic length l_0 needs to be defined, which takes the submergence depth into account. The characteristic length is defined by

$$l_0 = \frac{4min(h,h_B)l_F^* y_0}{2min(h,h_B)+l_F^* y_0} + h - min(h,h_B). \qquad (2)$$

with the MRE height h_B and the unit length y_0. The first term of this equation is similar to the hydraulic diameter of a rectangular channel of a width equal to l_F, while the other terms express the submergence depth.

For emerged MRE, the sink term considering their density is proposed as

$$S(l_F^*)_{MRE,fit} = gh\frac{\partial h}{\partial x}\left[1-\left(\frac{l_0}{h}\right)^2\right] \qquad (3)$$

where, g is the acceleration due to gravity.

Statistical descriptors of the fit, calculated using Matlab scripts based on Grode et al. (2017), are shown in Figure 4. The results reveal excellent agreement between calculated sink terms from CFD results and the fitted sink term.

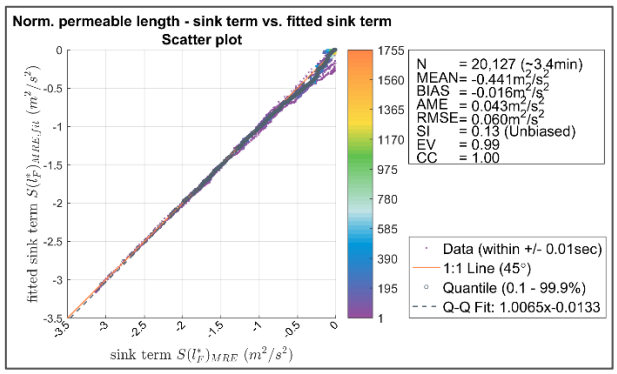

Figure 4 – Sink term data $S(l_F^*)_{MRE}$ vs calculated sink term $S(l_F^*)_{MRE,fit}$ according to Eq 3 over entire range of variations of normalized permeable length l_F^* for emerged MRE.

The sink term was consequently extended to incorporate also the effects originating from the relative height, the arrangement and the shape of the MRE. The finally derived sink term $S_{MRE,fit} = f\left(l_F^*, h_B^*, C_D, \Psi_B, Re, Fr, Eu, gh\frac{\partial h}{\partial x}, \frac{\partial}{\partial x}\frac{p(x)^2}{h}\right)$ was then implemented in COMCOT and tested against experimental data from Park et al. (2013).

REFERENCES

Grode, P., et al. (2017): Internal DHI Matlab Toolbox.

Leschka, S., Oumeraci, H., Larsen, O. (2014): "Hydrodynamic Forces on a Group of Three Emerged Cylinders by Solitary Waves and Bores: The Effect of Cylinder Arrangement and Distances", Journal of Earthquake and Tsunami, WORLD SCIENTIFIC, vol. 8 (3), 144005 (36 pages).

Park, H., Cox, D.T., Lynett, P.J., Wiebe, D.M., Shin, S. (2013): "Tsunami inundation modeling in constructed environments: A physical and numerical comparison of free-surface elevation, velocity, and momentum flux" Coastal Engineering, ELSEVIER, vol. 79, pp. 9-21.

Wang, X. (2008): "User manual for COMCOT version 1.7 (first draft)".